ELSEVIER

Polymer 40 (1999) 2537–2545

polymer

A small angle scattering study of dendrimer–copper sulfide nanocomposites

N.C. Beck Tan[a,*], L. Balogh[b], S.F. Trevino[a,c], D.A. Tomalia[b], J.S. Lin[d]

[a]*Army Research Laboratory, AMSRL-WM-MA/ Bldg. 4600, APG, Aberdeen, MD 21005, USA*
[b]*Michigan Molecular Institute, Midland, MI 48640, USA*
[c]*National Institute of Standards and Technology, Gaithersburg, MD 20899, USA*
[d]*Oak Ridge National Laboratories, Oak Ridge, TN 37831, USA*

Received 7 May 1998; revised 18 June 1998; accepted 18 June 1998

Abstract

Dendrimers are a new class of three-dimensional, man-made molecules produced by an unusual synthetic route which incorporates repetitive branching sequences to create a unique novel architecture. Exceptional features of the dendritic architecture include a high degree of structural symmetry, a density gradient displaying an intra-molecular minimum value and a well defined number of terminal groups which may be chemically different from the interior. The combination of these features creates an environment within the dendrimer molecule which facilitates trapping of guest species. Recently, dendritic polymers have been used as soluble templates/unimolecular reactors from which nano-clusters of inorganic compounds or elements can be synthesized. The basic concept involves using dendrimers as hosts to pre-organize small molecules or metal ions, followed by a simple in situ reaction which will immobilize and stabilize domains of atomic or molecular guest components (inorganic compounds as well as elemental metals). In one of these examples poly(amidoamine) (PAMAM) dendrimers have been used, to attract copper(II) ions inside the macromolecules where they are subsequently reacted with solubilized H_2S to form metal sulfides. These organic/inorganic, dendrimer-based hybrid species have been termed 'nanocomposites' and display unusual properties. For example, solubility of the nanocomposites is determined by the properties of the host dendrimer molecules. This allows for solubilization of the inorganic guest compounds in environments in which they are inherently insoluble. Since it has been established that there is no covalent bond between host and guest, these observations suggest that the inorganics are physically and spatially restricted by the dendrimer shell. However, this structure has not been verified. In this investigation a preliminary understanding of the physical structure of these dendrimer-based nanocomposites was sought. A model system of PAMAM dendrimer–copper sulfide nanocomposites was studied in various stages of its formation using a combination of small angle X-ray and neutron scattering experiments. The results suggest that little perturbation of the dendritic species occurs on complexation, but indicate that a secondary super-molecular aggregation phenomena occurs within nanocomposite solutions.

Keywords: Dendrimers; Nanocomposites; SANS

1. Introduction

As the chemical synthesis of dendritic polymers matures, the search for applications is becoming increasingly active. Successful exploitation of the technology will necessarily take advantage of the unique, ultra-branched architecture of these molecules, which lends them many properties which are distinctly different from those of their linear analogs. Features which make the dendrimers attractive for a variety of applications include an unprecedented control over composition and architecture, a minimum in their intra-molecular density gradient and a high number of end-groups which may be chemically different from the interior. The combination of these features creates an environment within the dendrimer molecule which facilitates trapping of guest species [1–6] and offers the potential for exploitation in applications ranging from drug delivery to pigmentation of olefins to microelectronics.

Recently, we have been able to use dendrimers as soluble, unimolecular reactors in which nano-clusters of metallic species [7] or inorganic compounds can be synthesized [8,9]. The natural chelating ability of polyamidoamine (PAMAM) dendrimers with tertiary nitrogen branch points has been used to attract metal ions into the dendrimer interior, and solution chemistry has subsequently been employed

* Corresponding author.

0032-3861/99/$ - see front matter
PII: S0032-3861(98)00491-1

to convert the complexed metal ions into compounds. These organic/inorganic dendrimer-based hybrid species have been termed 'nanocomposites' to distinguish them from metallo-dendrimers and metallo-dendritic structures in which a metal ion or complex forms part of the 'backbone' of the polymer [10–13]. Early investigations suggest that the inorganic clusters are physically linked with the dendrimer templates, and that the solubility of these molecular nanocomposites is controlled by the polymer [8]. Thus, it is possible to solubilize conventionally insoluble inorganic compounds in water or other solvents using dendritic hosts. Conceptually, these materials have tremendous potential for applications such as catalysts or molecular devices, however, little is understood about their structure.

In this investigation we seek to gain preliminary understanding of the structure of the solubilized molecular nanocomposites in various stages of their formation. A model system of PAMAM dendrimer and copper sulfide was chosen for study. Its structure was probed using small angle scattering techniques which are uniquely suited to the study of solubilized particles in the nanometer size range. A combination of small angle neutron scattering (SANS) and small angle X-ray scattering (SAXS) have been employed to examine: (a) the dimensions of dendrimer hosts and changes induced therein by complex formation and the subsequent conversion of complexed ions to immobilized conventionally insoluble compounds; (b) the size and state of complexed metal ions and metallic compounds trapped by the dendritic hosts; and (c) the propensity of the various systems for forming super-molecular structures.

2. Experimental

2.1. Materials

Ethylenediamine (EDA) core, generation 3.5 PAMAM dendrimers [14] were purchased from Dendritech, Inc., deuterium oxide (100%) and copper(II) acetate were obtained from Aldrich Chemical, and used as received. Hydrogen sulfide gas was purchased from Matheson, Inc.

2.2. Nanocomposite synthesis

Nanocomposite synthesis [8] was accomplished in two steps: (1) dendrimer complex formation, and (2) immobilization reaction. A fourth generation EDA-core tris(hydroxymethyl)aminomethane terminated [15–17] dendrimer having $M_n = 18\,214$ g/mole and 192 hydroxyl endgroups [8,9,18] was used as the host molecule. This modified dendrimer, designated G4.T, is completely soluble in water and has tertiary nitrogens only in its interior. Complexation (Step 1) was accomplished by adding copper(II) acetate to a dilute solution of PAMAM G4.T dendrimer in deuterated water (D_2O), in a ratio allowing for 15 copper ions per dendrimer molecule which is slightly below the PAMAM G4.T measured maximum complexing capacity [7]. The complex was subsequently isolated as a blue solid, and then redissolved in D_2O to form a 1.5% solution. Nanocomposite synthesis was completed by reacting the $[(CuAc_2)_{15}$–PAMAM G4.T] dendrimer complex in a 1.5% aqueous, solution with a slow stream of hydrogen sulfide gas (Step 2). After converting the blue copper(II) complex solution to the dark brown but transparent $\{(CuS)_n$–PAMAM G4.T} nanocomposite solutions, the sulfide nanocomposite stock solutions were degassed with nitrogen. Nanocomposites prepared in this manner are soluble in water up to 10% concentration, in contrast to pure CuS which displays negligible solubility ($K_{sp} = 6.3 \times 10^{-36}$) in water [19]. Synthetic details of the dendrimer nanocomposite preparation and characteriazation are discussed elsewhere [9,18].

2.3. Small angle scattering measurements

Solutions of the $[(CuAc_2)_{15}$–PAMAM G4.T] copper complex and the $\{(CuS)_{15}$–PAMAM G4.T} nanocomposites in D_2O were diluted from the 1.5% solutions used in synthesis to concentrations of 0.1, 0.3, 0.5 and 0.8% for scattering measurements. After the final dilution, solutions were divided into two identical sets (one for SANS, one for SAXS) and sealed in vials under nitrogen atmosphere for transport to experimental facilities. Samples were transferred from nitrogen sealed vials into closed cells for measurements conducted 2–3 days after their preparation (SAXS) or 4–6 days after their preparation (SANS).

Samples for SANS measurements were transferred into optical quality quartz cells with 1 mm path length. All SANS studies were performed at the Center for Neutron Research at the National Institute of Standards and Technology. Measurements were made using the 30 m SANS instrument with neutron wavelength of $\lambda = 7$ Å and wavelength spread of 0.015. Three different sample-to-detector distance configurations were employed to collect data over a wide range of scattering vector. All data were corrected for empty quartz cell scattering, electronic background and detector uniformity, and converted to an absolute intensity scale using secondary standards. Before analysis, the data were further corrected by subtracting the contributions from solvent scattering and incoherent background.

Samples for SAXS measurements were transferred into closed cells with polyimide windows and 1 mm path length. All SAXS studies were performed at the 10 m SAXS Facility at Oak Ridge National Laboratory [20] using copper radiation with $\lambda = 1.54$ Å and pinhole collimation of the incident beam. All data were corrected for empty cell scattering, solvent scattering, electronic background and detector uniformity.

3. Theoretical background

The small angle scattering intensity, $I(\mathbf{Q})$, from an assembly of particles dispersed in a solvent may be represented by the expression:

$$I(\mathbf{Q}) = NK_iP(\mathbf{Q})S(\mathbf{Q}) \quad (1)$$

where $\mathbf{Q} = (4\pi/\lambda)\sin(\theta/2)$ is the momentum transfer vector, or 'scattering vector', corresponding to the scattering angle (θ) of radiation having wavelength λ, N is the number of scattering particles, K_i is a contrast factor for radiation of type i, $P(\mathbf{Q})$ is the intraparticle scattering function for a single particle, and $S(\mathbf{Q})$ is a scattering function for interparticle correlations [21,22]. When the particles are non-interacting and in dilute solution, the intraparticle contribution dominates the scattering. Under these conditions the function $S(\mathbf{Q})$ approaches unity, simplifying Eq. (1) to:

$$I(\mathbf{Q}) = NK_iP(\mathbf{Q}) \quad (2)$$

Thus, the form of the scattered intensity, $I(\mathbf{Q})$, from a dilute solution of non-interacting particles as a function of the scattering vector, $\mathbf{Q}$, is defined by the function $P(\mathbf{Q})$, while the magnitude of the scattered intensity is controlled by K_i.

The contrast factor, K_i, gives a measure of the difference between the scattering power of a particle and the scattering power of the surrounding medium. Because X-rays interact with the electron cloud of atoms, the X-ray scattering power or 'X-ray scattering length' of a given species is directly related to its electron density (no. electrons/unit volume). Elements with high atomic number (i.e. Cu, S) will scatter X-rays more strongly than elements with small atomic number (i.e. H^1, H^2, C, N, O). Therefore, X-ray contrast (K_X) may be generated by complexation or incorporation of inorganic species into particles dispersed in an organic solvent. Unlike X-rays, neutrons interact with the nuclei of atoms. Neutron scattering lengths may take either positive or negative values, and are often very different for different isotopes of a given atomic species. For example, the neutron scattering length for hydrogen is $b_c(H^1) = -3.739$ fermi, while the neutron scattering for deuterium is $b_c(H^2) = 6.671$ fermi [23]. This isotopic discrepancy in scattering lengths is the basis for deuterium labeling in the study of organic species using neutrons; it is the value of $b_c(H^1)$ which is unusual, other elements comprising common organic species (C, N, O, H^2, S), as well as many metallic ions (Cu) have positive neutron scattering lengths in the range of 2–10 fermi [23]. In the present study, neutron contrast was manipulated by using deuterated solvents, generating significant neutron scattering contrast between the solvent and the hydrogenated, dendrimer-based particles. Applying both X-ray and neutron scattering techniques to the same series of samples allowed for an independent probe into the behavior of the dendrimer molecules (the hydrogen-rich components of the system) using SANS, and the distribution of the metallic components of the system (Cu^{2+} ions and CuS domains) using SAXS.

Returning to Eq. (2), one sees that while it is K_i that defines which species in the system constitutes a particle, all of the information regarding the structure of the particle is contained in $P(\mathbf{Q})$. In this study, the goal is to extract the radius of gyration, R_g, for a given particle (dendrimer, complex or nanocomposite) from the scattered intensity, which gives a measure of the mean square distance of the scattering centers within the particle from its center of gravity and therefore is related to particle size. For scattering from a dilute solution of non-interacting particles, in the limit of low $\mathbf{Q}$ where $\mathbf{Q}R_g \ll 1$, the scattered intensity, $I(\mathbf{Q})$ is simply related to $(R_g\mathbf{Q})^2$. Practical considerations generally prohibit the collection of scattering data in the extreme limit of low $\mathbf{Q}$, and therefore proper estimation of R_g from experimental data requires an appropriate choice of the analytical method [21,22]. For scattering from a collection of scattering centers which are assembled into a particle resembling a sphere, the Guinier method is appropriate for analysis of scattering data [24], and the function $P(\mathbf{Q})$ takes the form:

$$P_{\text{Guinier}}(\mathbf{Q}) = \exp\left[-\frac{\mathbf{Q}^2R_g^2}{3}\right] \quad (3)$$

Combining Eqs. (2) and (3) allows for the extraction of R_g from the slope of a plot of $\ln(I(\mathbf{Q}))$ versus $\mathbf{Q}^2$. Several recent studies have demonstrated that the scattering from dendrimers in solution may be approximated by the scattering from spherical particles [24–29] and that the Guinier method is appropriate for the analysis of experimental scattering data from fourth generation dendrimers [28].

4. Results and discussion

4.1. Particle interactions and contrast

Small angle neutron scattering curves from a concentration series of PAMAM G4.T dendrimers in deuterated water are shown in Fig. 1. The contrast giving rise to scattering in these solutions is generated by the difference in scattering length density between the hydrogenated dendrimer and the deuterated solvent. Clearly, a maximum begins to develop in the scattering from PAMAM G4.T in the concentration range between 0.3 and 0.8% by weight, indicating that intermolecular interactions are occurring in solution. Due to the presence of these interactions, all analysis of data from pure PAMAM G4.T in solution was performed on scattering curves from solutions with concentration $\leq 0.5\%$, which displayed no evidence of interparticle interactions. Electrostatic interactions between dendrimer molecules in solution have been observed previously in the scattering from aqueous solutions of $-NH_2$ terminated PAMAM dendrimers [30]. However, the modified PAMAM G4.T dendrimers used in this study contain only hydroxyl terminal groups, the intermolecular interactions

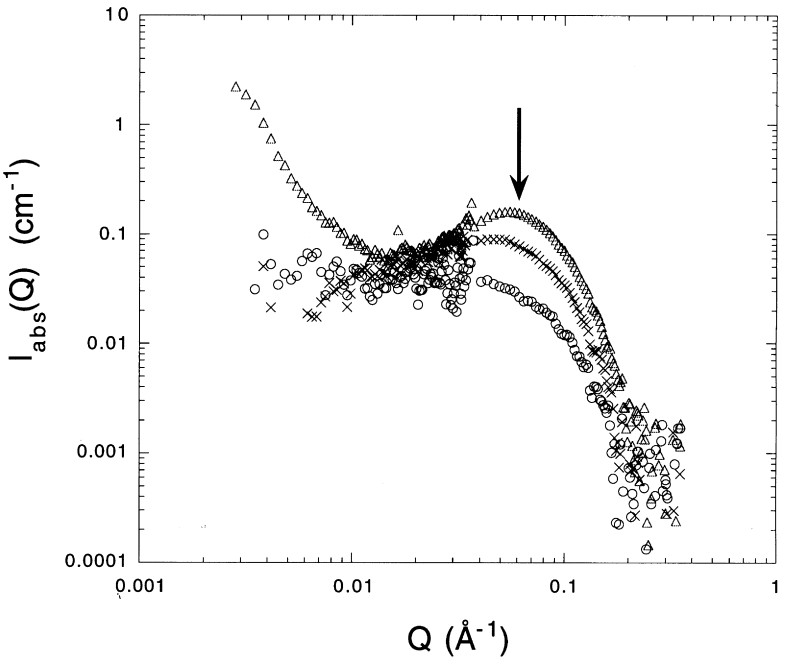

Fig. 1. SANS data from solutions of PAMAM G4.T dendrimer in D_2O: (○) 0.3 wt%; (×) 0.8 wt%; (Δ) 1.5 wt%. Arrow indicates position of interparticle interference maximum (see text).

of which should be screened in aqueous solution. The appearance of a maximum in the PAMAM G4.T scattering curves at low concentration is therefore an indication of strong intermolecular interactions between species present within the dendrimer interior. In contrast, the SANS curves from $[(CuAc_2)_{15}$–PAMAM G4.T] solutions did not show evidence of interparticle interactions at concentrations up to 1.5% by weight (Fig. 2), indicating effective screening of interparticle interactions by the addition of salt, behavior which is similar to that which has been observed previously for primary amine terminated dendrimers [30].

The scattered X-ray intensity versus scattering vector curves for PAMAM G4.T dendrimer and $[(CuAc_2)_{15}$–PAMAM G4.T] solutions accumulated over 1 h are displayed in Fig. 3. While the intensity of X-radiation

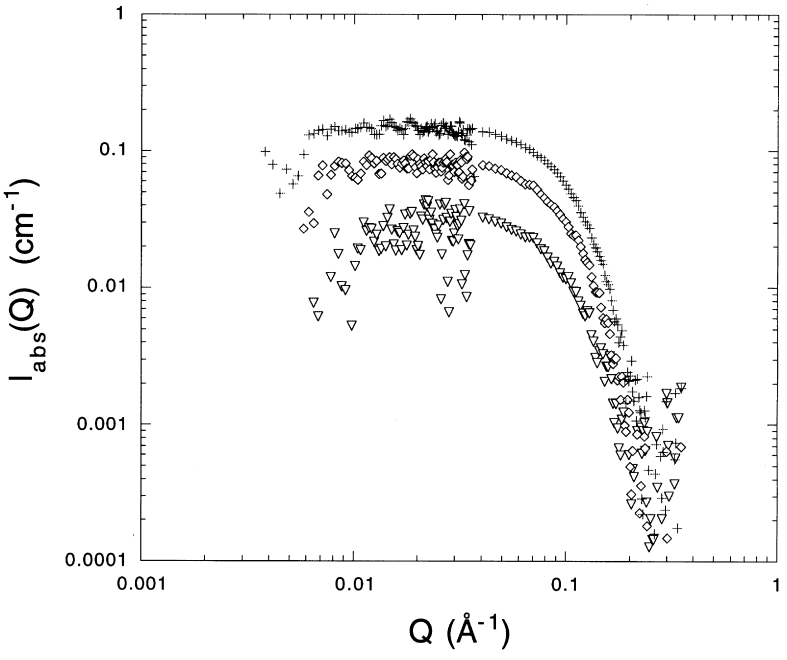

Fig. 2. SANS data from solutions of $[(CuAc_2)_{15}$–PAMAM G4.T] complex in D_2O: (▽) 0.3 wt%; (◇) 0.8 wt%; (+) 1.5 wt%.

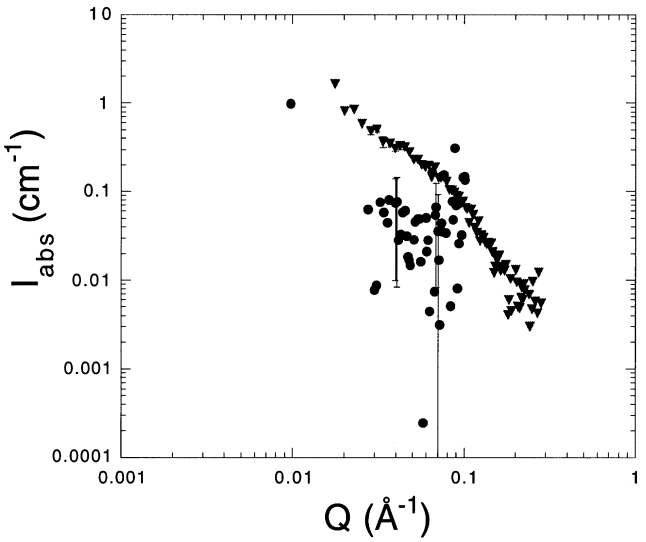

Fig. 3. SAXS data from 0.3 wt% solutions of (●) PAMAM G4.T dendrimer in D_2O, and (▼) [$(CuAc_2)_{15}$–PAMAM G4.T] complex in D_2O. Data collected over 1 h. Representative error bars are included on a limited number of data points.

scattered from the pure dendrimer is indistinguishable from background noise, the SAXS intensity for the solutions of dendrimer Cu^{2+} complex in water is readily measurable, verifying the association of the metal ions with the dendrimer molecules. These results coupled with the results of previous electron paramagnetic resonance studies [1] indicate that the Cu^{2+} ions are associated with internal, tertiary amino groups of the surface modified PAMAM G4.T dendrimers.

4.2. Analysis of dendrimer complexes

Plots of ln[I(**Q**)] versus $\mathbf{Q}^2$ from PAMAM G4.T solutions and [$(CuAc_2)_{15}$–PAMAM G4.T] solutions show a linear relationship in the low **Q** region, indicating that a Guinier analysis of the data is appropriate for the extraction of radii of gyration (Fig. 4). The R_g values calculated from the slope of the ln[I(**Q**)] versus Q^2 plots (Eqs. (2) and (3)) are listed in Table 1. The results of the Guinier analysis indicate that R_g (G4.T)∼19 Å, which, as expected, is similar to sizes reported previously for unmodified primary amine terminated G4.0 PAMAM dendrimers [28,31]. The agreement between R_g values extracted from the PAMAM G4.T and [$(CuAc_2)_{15}$–PAMAM G4.T] complex solutions shows that complexation does not alter the physical size of the dendrimer molecules significantly.

Comparison of R_g values measured from PAMAM G4.T solutions and [$(CuAc_2)_{15}$–PAMAM G4.T] solutions using SAXS ($R_{g,X}$) and SANS ($R_{g,N}$) indicates that there is no difference between the values obtained from the two techniques to within the uncertainty of the measurement analysis (typically ∼5–10%). The agreement between $R_{g,X}$ and $R_{g,N}$ suggests that the scattering centers giving rise to the X-ray scattering are distributed about the molecule in a similar way to the scattering centers giving rise to neutron scattering. This, in turn, which implies that there is no preferential positioning of Cu^{2+} atoms within the PAMAM dendrimer

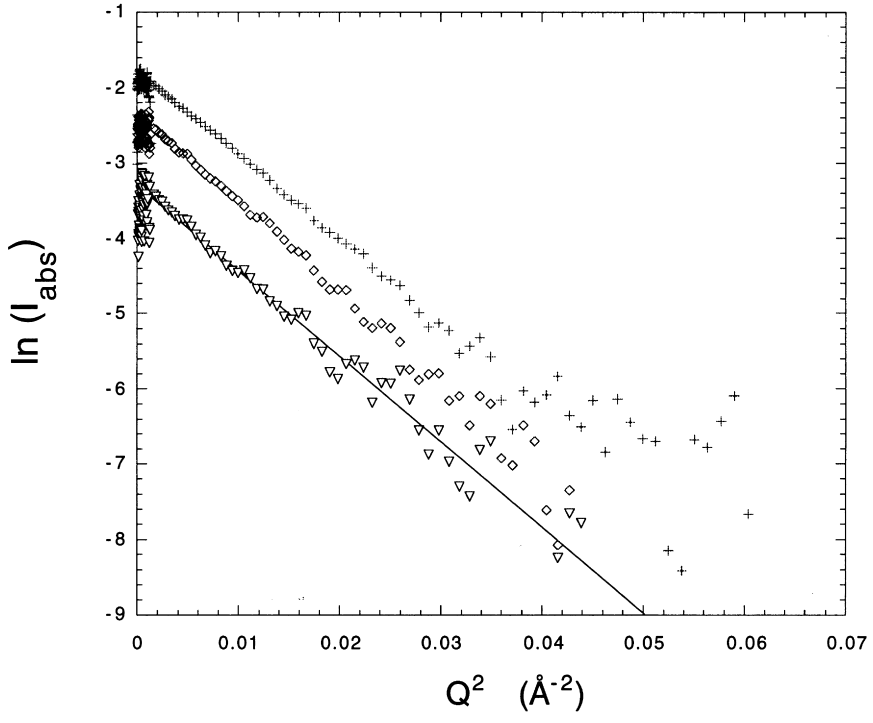

Fig. 4. Guinier plots of SANS data from G4.T dendrimer/copper acetate complexes[$(CuAc_2)_{15}$–PAMAM G4.T]: (∇) 0.3 wt%; (◇) 0.8 wt%; (+) 1.5 wt%. For the linear fit shown, (———) slope = −113.6 $Å^2$, correlation coefficient R^2 = 0.9751.

Table 1
Radii of gyration measured for endgroup modified PAMAM G4.T dendrimers and [$(CuAc_2)_{15}$–PAMAM G4.T] complexes

Particle	C (wt%)	$R_{g,N}$ (Å)	$R_{g,X}$ (Å)
PAMAM G4.T	0.3	18.8	19.2[a]
[$(CuAc_2)_{15}$–PAMAM G4.T]	0.3	18.7	–
[$(CuAc_2)_{15}$–PAMAM G4.T]	0.8	18.9	–
[$(CuAc_2)_{15}$–PAMAM G4.T]	1.5	18.3	19.2

[a] Due to low X-ray contrast between PAMAM G4.T and water, it was possible to collect a measurable signal for analysis only by increasing measurement time to more than 10 h.

host. This behavior is in contrast to the behavior of polyethyleneimine dendrimer complexes in which preferential association of metal ions with terminal amine groups has been observed [32].

4.3. Analysis of dendrimer/copper sulfide nanocomposites

Though complexation of the dendrimers with Cu^{2+} seems to leave the molecular dimensions unperturbed, the conversion of the [$(CuAc_2)_{15}$–PAMAM G4.T] complexes to {$(CuS)_{15}$–PAMAM G4.T} nanocomposites results in a structural change to the scattering particles, which is evident from the small angle scattering patterns (Figs. 5 and 6). The scattering behaviors of the dendrimer, dendrimer complex, and dendrimer nanocomposite solutions in the high **Q** region are very similar, indicating that the contribution from the individual dendrimer molecules manifests itself in this range. However, both SANS and SAXS patterns from the G4.T/CuS nanocomposite solutions show evidence of enhanced scattering in the low **Q** range which is not present in the scattering from the dendrimer or copper complex solutions. Emergence of this lower **Q** feature in the scattering from the nanocomposite solutions is indicative of the formation of larger multi-dendrimer aggregates in this system. The Guinier plots of the SANS and SAXS data from {$(CuS)_{15}$–PAMAM G4.T} nanocomposites clearly show the two distinct regions as well (Fig. 7). The linear relationship between ln[I(**Q**)] and $\mathbf{Q}^2$ in each region indicates that a Guinier analysis is valid, and a radius of gyration for each feature may be extracted from the slope of its corresponding linear region provided the analysis is performed over a **Q** range in which $\mathbf{Q}R_g$ is near unity.

Particle radii of gyration extracted from the higher **Q** region in which the single molecule features are prevalent are given in Table 2. There is a significant difference in the single molecule feature's $R_{g,X}$ and $R_{g,N}$ values, extracted from the nanocomposite solution scattering, indicating a difference in the distributions of the X-ray and neutron scattering centers about the individual dendrimer–CuS hybrid molecules. The value of $R_{g,N}$ (~19 Å) obtained from analysis of the single molecule scattering region for the {$(CuS)_{15}$–PAMAM G4.T} nanocomposite agrees with the values measured for PAMAM G4.T and [$(CuAc_2)_{15}$–PAMAM G4.T], indicating that the organic part of the nanocomposite—the dendrimer molecule—remains unchanged during the conversion from pure

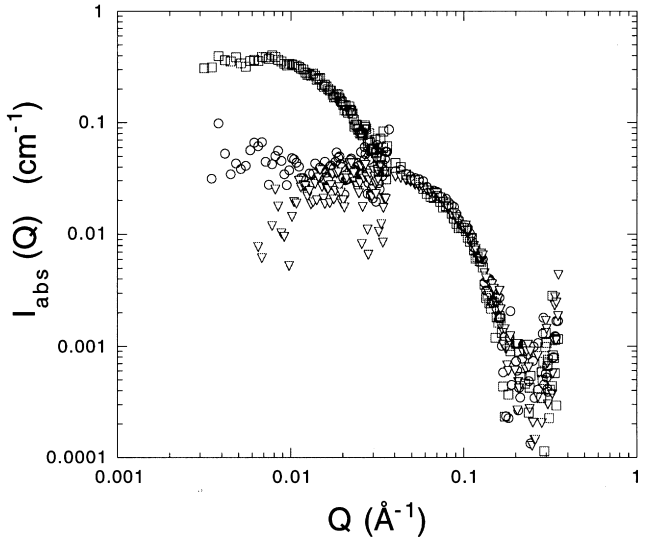

Fig. 5. SANS data from (○) PAMAM G4.T dendrimer, (▽) [$(CuAc_2)_{15}$–PAMAM G4.T] complex, and (□) {$(CuS)_{15}$–PAMAM G4.T} nanocomposite in D_2O solution.

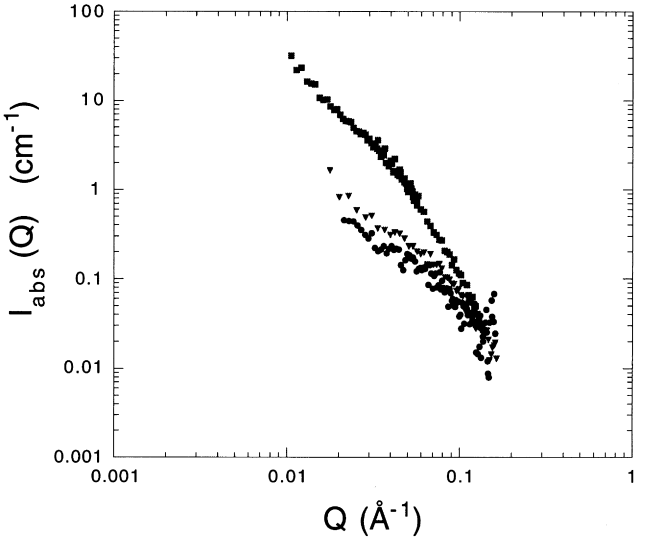

Fig. 6. SAXS data from (●) PAMAM G4.T dendrimer*, (▼) [$(CuAc_2)_{15}$–PAMAM G4.T] complex, and (■) {$(CuS)_{15}$–PAMAM G4.T} nanocomposite in D_2O. * G4.T data collected for 10 h.

Table 2
Radii of gyration for {$(CuS)_{15}$–PAMAM G4.T} nanocomposites. Individual dendrimer feature and supermolecular aggregates

Feature	$R_{g,N}$ (Å)	$R_{g,X}$ (Å)	$\mathbf{Q}R_g$ range	R_N sphere (Å)	R_X shell (Å)	Number of dendrimers
Higher **Q**—single molecule	18.8	23.7	1.0–3.5 (N), 1.5–3.2 (X)	24.3	23.7	1
Lower **Q**—aggregate	90	–	0.5–1.9 (N)	116	–	~50–110[a]

[a] A calculation of the exact number of dendrimer molecules in a super-molecular aggregate cannot be made without assuming a particular type of molecular packing within the cluster. A packing fraction of 50% would suggest ~54 dendrimers per aggregate. Complete space-filling (100% packing fraction) would suggest ~108 dendrimers per aggregate.

dendrimer to Cu^{2+} complex to CuS nanocomposite. However, the X-ray scattering measurements show that $R_{g,X}$ of the single molecule scattering feature increases significantly on conversion of the complex to the nanocomposite, indicating a change in the distribution of the inorganic components within the dendrimer molecules on conversion of the G4.T/Cu^{2+} hybrid to the G4.T/CuS hybrid.

If the X-ray and neutron scattering centers were each distributed evenly about a spherical particle, the fact that $R_{g,X}$ {$(CuS)_{15}$–PAMAM G4.T} is greater than $R_{g,N}$ {$(CuS)_{15}$–PAMAM G4.T} would suggest that a water soluble CuS particle is formed on conversion of the Cu^{2+} complex which is larger than a single dendrimer molecule. This is highly improbable, given the insolubility of CuS in water and the Cu/dendrimer ratio stoichiometry in the system (~15 CuS molecules per D~50 Å dendrimer molecule). Similarly, the fact that $R_{g,X}$ is greater than $R_{g,N}$ negates the possibility that the CuS molecules are condensed in a compact spherical region within a single, dendrimer host molecule. In order to interpret the physical meaning of these results, it is necessary to consider the relationship between the dimensions of specific geometrical objects and their radii of gyration. The radius of the dendrimer molecules which comprise the smallest unit of the nanocomposite and are known to behave as spherical particles in solution [24–29] can be calculated from

$$R_{\text{PAMAM sphere,N}} = \sqrt{(5/3)}R_{\text{g,N, HighQ}} = 24.3\text{Å}$$

From the X-ray experiments, the measured $R_{g,X,\ \text{High Q}} \sim 24$ Å would correspond to a spherical CuS particle with $R_{\text{sphere,X}} \sim 31$ Å in diameter, a non-physical result, as noted above. In considering alternate geometrical shapes with spherical symmetry, one finds that an X-ray scattering center in the shape of a thin, spherical shell of CuS as measured by X-rays would have, $R_{\text{shell,X}} = R_{g,X} = 23.7$ Å. This value, $R_{\text{CuS shell,X}} \sim 24$ Å, is in good agreement with the radius of the spherical dendrimer molecule which hosted the CuS reactants, $R_{\text{PAMAM sphere,N}} \sim 24$ Å (Table 2). The agreement implies that on conversion to the neutral CuS species, the Cu^{2+} ions from the complex which are located throughout the dendrimer molecules redistribute and become localized near the periphery of the dendrimer molecule in a region whose shape approximates a thin, spherical shell. The proposed structure is illustrated schematically in Fig. 8 (left). The formation of such a structure is reasonable, given that the spherical symmetry of dendrimers has been established and it is not unlikely that the conversion of internally complexed Cu^{2+} ions to neutral CuS compounds by reaction with a gas introduced through the solvent should take place in the peripherial region of the PAMAM dendrimer.

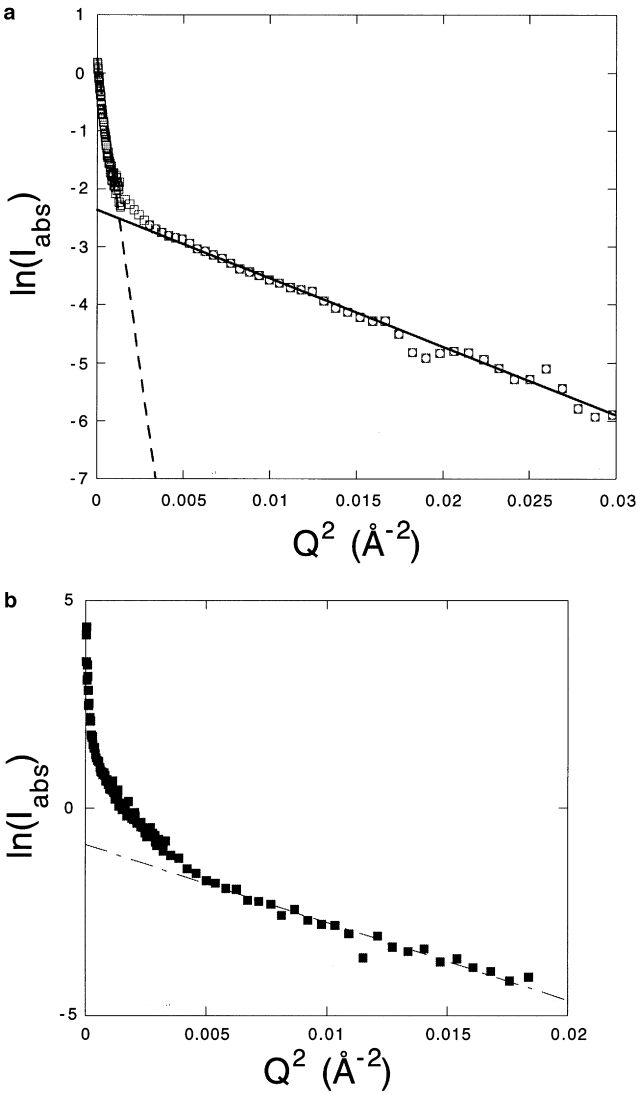

Fig. 7. Guinier plots of (a) SANS data and (b) SAXS data from {$(CuS)_{15}$–PAMAM G4.T} nanocomposite solutions in D_2O. (a) (———) slope = −118.0 Å^2, correlation coefficient $R^2 = 0.9897$; (- - -) slope = −2981. Å^2, correlation coefficient $R^2 = 0.9919$. (b) (—— — ——) slope = −187.9 Å^2, correlation coefficient $R^2 = 0.9634$.

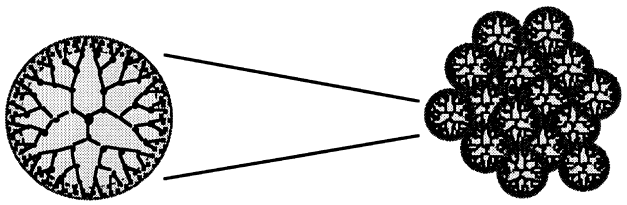

Fig. 8. Schematic representation of the model nanomolecular composite structure derived from SANS and SAXS measurements. Left, individual dendrimer molecule with CuS trapped at its periphery. Right, multimolecular cluster of individual dendrimer/CuS particles.

An analysis of the enhanced low **Q** scattering from the nanocomposite solutions remains. Due to experimental limitations, it was not possible to collect enough data points in the low **Q** region to perform an analysis of the low **Q** scattering feature from the X-ray data. However, sufficient data were collected in the low **Q** SANS range to allow for estimation of the size of the larger scattering feature from the neutron data. The Guinier analysis in this regime (Fig. 7(a), Table 2) indicates that the low **Q** scattering feature is contributed to by particles with $R_{g,N,\ low\ Q} \sim 90$ Å, or $R_{N,\ sphere,\ low\ Q} \sim 116$ Å. The size of these particles coupled with their scattering contributions in both SANS and SAXS suggest that they are soluble, supermolecular aggregates of dendrimer and copper sulfide large enough to contain 50–100 dendritic molecules. Given the nature of the SAS studies, it is not possible to determine without a doubt if the nanoclusters observed were formed immediately on sulfide formation, or are the result of slow aggregation in solution over time. However, it is likely that the aggregation phenomena are contributing strongly to the long-term destabilization of the insoluble inorganic species in the aqueous solution, occurring especially at higher concentrations.[1]

The combined results of the analyses of the SANS and SAXS data from the {$(CuS)_{15}$–PAMAM G4.T} nanocomposites in both the high **Q** and low **Q** regimes indicate that the nanocomposites exists in the physical form illustrated in Fig. 8, in which single dendrimers with copper sulfide molecules entrapped near their peripheriesy aggregate in solution forming clusters of 50 dendrimers or more. Future studies will be focused on the evaluation of stabilization schemes (surface modification, additives) on the structure and formation of dendrimer-based nanocomposites, on the structure of nanomolecular composites containing species other than copper sulfide, and on the development of appropriate sample preparation methods for applying complementary experimental techniques (TEM, SEC) to the study of these unique dendrimer-based nanocomposite materials.

[1] In an aqueous solution, stability of sulfide nanocomposites appears to be a function of both concentration and the degree of exposure to oxygen. (Sulfides are known to give polysulfides upon oxidation which may connect the dendrimer hosts.) It was observed that dilute solutions of sulfide nanocomposites in an inert or reductive atmosphere were stable for months, while a 10% solution of {$(Cu_2S)_{15.5}$–PAMAM G4.T} at room temperature displayed the visible signs of clustering after 1 day and gradually precipitated in 3 days.

5. Summary

The structure of nanomolecular {$(CuS)_{15}$–PAMAM G4.T} copper(II) sulfide–PAMAM dendrimer nanocomposites was studied by a combination of small angle X-ray and neutron scattering techniques. These inorganic/organic hybrid nanocomposites were prepared through the reaction of [$(CuAc_2)_{15}$–PAMAM G4.T] copper–dendrimer complexes in aqueous solution with hydrogen sulfide gas. The pure dendritic starting materials were found to exist as isolated, dispersed particles in dilute solution ($< 0.8\%$) having radii of gyration of ~19 Å. The physical size of the dendritic molecule was not perturbed by internal complexation of Cu^{2+} ions, or by the subsequent conversion of these ions into the neutral CuS species. Comparison between SANS and SAXS measurements of dendrimer–copper complexes and dendrimer–copper sulfide nanocomposites in solution indicate that the ions in the complexes are primarily distributed throughout the dendrimer molecules, but that conversion of the Cu^{2+} ions to neutral CuS molecules results in a redistribution of the inorganic species. The results imply that the CuS molecules in the nanocomposites are localized at the periphery of individual dendrimer molecules. In addition, there is strong evidence of aggregation in the nanocomposite system, which suggests that the stable form of the dendrimer/CuS hybrid species in solution is in supermolecular clusters containing more than 50 individual dendrimer–copper sulfide molecules.

Acknowledgements

Funding for this work was provided by the US Army Research Laboratory. Small angle scattering experiments were made possible through the use of facilities at the Center for Neutron Research at the National Institutes of Standards & Technology (SANS), and the High Temperature Materials Laboratory Center for Small-Angle Scattering Research at Oak Ridge National Lababoratory. The research was also supported by the Division of Materials Science, US Department of Energy under contract no. DE-AC05-96OR22464 with Lockheed Martin Energy Research Corporation. The assistance of Drs Tania Slawecki and Boualem Hammouda of the National Institutes of Standards & Technology with the neutron scattering experiments and their interpretation is gratefully acknowledged.

References

[1] Ottaviani MF, Montalti F, Turro NJ, Tomalia DA. J Phys Chem B 1997;101:158.

[2] Jensen et al. Science 1994;266:1226.
[3] Esfand et al. Pharm Sci 1996;2:157.
[4] Sayed-Sweet Y, Hedstrand DM, Spindler R, Tomalia DA. J Mater Chem 1997;9:1199.
[5] Cooper et al. Nature (London) 1997;389(6649):368.
[6] Dvornic PR, Tomalia DA. Current Opinion in Colloid & Interface Sci 1996;1:221.
[7] Balogh L, Tomalia DA. JACS, submitted.
[8] Balogh L, Swanson DR, Spindler R, Tomalia DA. ACS PMSE Preprints 1997;77:118.
[9] Balogh L, Tomalia DA. US Patent pending.
[10] Constable EC, Harverson P, Oberholzer M. Chem Comm 1996;15:1821.
[11] Serroni S, Denti G, Campagna S, Juris A, Ciano M, Balzani V. Angew Chem Int Ed Engl 1992;31:1493.
[12] Newkome GR, Cardullo F, Constable EC, Moorefield CN. J Chem Soc, Chem Commun 1993:925.
[13] Newkome GR, Gross J, Moorefield CN, Woosley BD. J Chem Soc, Chem Commun 1997;6:515.
[14] Tomalia DA, Dewald JR, Hall MJ, Martin SJ, Smith PB. First SPSJ Int Polym Conf, Kyoto, Japan, August 1984:65.
[15] Tomalia DA, Naylor AM, Goddard WA. Angew Chem Int Ed Engl 1990;29:138.
[16] Newkome GP, Nayak A, Behera RK, Moorefield CN, Baker GR. J Org Chem 1992;57:358.
[17] Newkome GP et al. J Am Chem Soc 1990;112:8458.
[18] Balogh L, Tomalia D. Advanced Materials, under review.
[19] Dean JA, editor. Lenlange handbook of chemistry, 12th ed. New York: McGraw-Hill, 1978.
[20] Wignall GD, Lin JS, Spooner S. J Appl Cryst 1990;23:241.
[21] Higgins JS, Benoit HC. Polymers and neutron scattering. Oxford: Clarendon Press, 1994.
[22] Feigin LA, Svergun DI. Structure analysis by small-angle X-ray and neutron scattering. New York: Plenum Press, 1987.
[23] Sears VF. Neutron News 1992;V3:26.
[24] Bauer BJ et al. ACS PMSE Preprints 1994;71:704.
[25] Bauer BJ, Hammouda B, Briber RM, Tomalia DA. ACS PMSE Preprints 1993;69:341.
[26] Bauer BJ et al. ACS PMSE Preprints 1997;77:87.
[27] Amis EA, Topp A, Bauer BJ, Tomalia DA. ACS PMSE Preprints 1997;77:183.
[28] Prosa TJ et al.. J Polym Sci Polym Phys 1997;35:2913.
[29] Thiyagarajan P, Zeng F, Ku CY, Zimmerman SC. J Mater Chem 1997;7:1221.
[30] Bauer BJ, Briber RJ, Hammouda B, Tomalia DA. ACS PMSE Preprints 1992;67:428.
[31] Dvornic PR, Tomalia DA. Starburst dendrimers techology review. Midland, MI: Dendritech, Inc., 1995.
[32] Bosman AW, Schenning APH, Janssen RAJ, Meijer EW. Chem Ber/Recueil 1997;130:725.